

Toxic Solid Waste Disposal Container Weight Variations Modelling Considering Instances Of Vehicle Encounter With Speed Bump Obstruction

Eyo Akabom Joseph¹

Department of Mechanical and Aerospace Engineering,
University of Uyo, Uyo, Akwaibom State-Nigeria

Aniekan Offiong²

Department of Mechanical and Aerospace Engineering,
University of Uyo, Uyo, Akwaibom State-Nigeria

Markson, I. E.³

Department of Mechanical Engineering
University of Uyo, Uyo Akwa Ibom State, Ngeria
idorenyinmarkson@uniuyo.edu.ng

Ozuomba Simeon⁴

Department of Electrical/Electronic and Computer Engineering
University of Uyo, Uyo Akwa Ibom State, Ngeria
simeonozuomba@uniuyo.edu.ng

Alexander Aniekan Offiong⁵

Department of Mechanical and Aerospace Engineering,
University of Uyo, Uyo, Akwaibom State-Nigeria

Abstract— In this paper, toxic solid waste disposal container weight variations modelling considering instances of vehicle encounter with speed bump obstruction is presented. This is part of a wider study on tampering monitoring for solid toxic waste disposal management in the oil and gas industry. The work is meant to provide insight into the variation in the solid waste container weight, the lift force and lift height of the waste container as the vehicle decelerates towards the road bump and as the vehicle hits the road bump while in motion. The analytical models are further modelled in Simulink software and several simulations are conducted using sample solid waste container capacity, sensors, and vehicle motion parameters. The simulation results show that in one instance the vehicle approached the road bump having height of 0.04m with deceleration of 3km/hr². The weight of the solid waste container as captured by the sensors was over 8 times the actual weight. This sharp momentary rise in the container weight occurred the moment the vehicle hits the road bump and the container lifted up slightly and then landed back on the weight monitoring sensors. There

were subsequent momentary sporadic rise and fall in the container weight during the vehicle encounter with the road bump but the weight returned to stable value at about 15 seconds after the encounter with the road bump. The rise and fall in the container weight is essential in monitoring tampering of the toxic solid waste while on transit. As such, proper estimation of the nature of variations in the container weight during encounter with road bump is essential to avoid false alarm of tampering due to container weight variations in such situations.

Keywords— Toxic Solid Waste, Tampering Monitoring Mechanism, Waste Disposal Management, Sensors

1. INTRODUCTION

In recent years, there has been growing adoption of smart technologies in diverse fields [1,2,3]. Accordingly, waste disposal systems are being modernized to take advantage of the emerging smart technologies. The smart technologies will facilitate monitoring of waste disposal and provide real-time feedback on the condition of the

waste while on transit from the pick-up point to the destination point [4,5,6]. Such system is specifically important for monitoring of solid toxic waste disposal in the oil and gas industries. The system when applied can be used to monitor tampering of the toxic waste while being transported from the oil company premises to the destination point where experts will properly dispose the waste [7,8].

In this paper, the focus is to address one aspect of the challenges that may arise and make it difficult for the smart system to accurately detect tampering incidence. Notably, the model for monitoring tampering of the waste uses weight sensors and velocity sensors to monitor the toxic waste container while being conveyed by the vehicle [9,10,11,12]. The analytical models capture the variations in the waste container weight and velocity under different conditions. Based on proper modelling of the various possible conditions that the waste container may experience, it is possible to determine when tampering has occurred or when the conditions can be attributed to other issues other than tampering of the waste.

Accordingly, in this paper, the mathematical models that capture the various parameters pertaining to the weight, velocity, acceleration, de-acceleration and other forces that are likely to occur when the vehicle conveying the solid waste encounters obstruction like road bump are presented. The parameters are also modeled in MATLAB/SIMULINK environment. The system is simulated to distinguish incidence of encounter with obstruction from incidence of tampering of the solid waste while in being transported to the destination. The essence of the study is to avoid or minimize false tampering alert when the vehicle encounters obstruction along the road.

2. METHODOLOGY

In order to effectively automate the monitoring and management of anti-tampering of the solid waste while being transported, it is important to model the vehicle motion parameter under different conditions. One of the condition considered in this study is the vehicle encounter with road bump while in motion. When the vehicle conveying the waste container encounters obstruction such as road bump, the vehicle is expected to slow down, cross the bump at a minimal velocity and then accelerates again to gain speed. This work therefore focus on developing the models for the velocity and weight of the toxic waste container during trailer encounter with speed bumps obstruction while in motion

2.1 Encounter with Speed bumps

At this condition, the vehicle decelerated before scaling the speed bumps causing a sharp rise in the weight of the container as a result of turbulence of the toxic waste before normalizing. The velocity reduced the increased after crossing the bump. The model for the deceleration is shown in Equation 1.

$$A_{dec} = \frac{F_d t}{M_T + \frac{J_e}{r^2}} \quad (1)$$

Where A_{dec} represents the deceleration of the vehicle, F_d represents the force towards the vehicle deceleration, M_T represents the total mass of the vehicle (including the toxic waste), r represents the radius of the wheel of the vehicle, J_e represents the equivalent inertia of the rotational wheel of

the vehicle. Hence the equivalent total mass (M_e) of the vehicle is shown in Equation 2.

$$M_e = \frac{M_T + J_e}{r^2} \quad (3)$$

The actual deceleration force accounting for the air resistance, drag force and force of gravity is shown in Equation 4.

$$F_{decc} = F_d - F_a - F_{ro} - F_{gr} \quad (4)$$

Where F_{decc} represents the actual deceleration force, F_d represents the deceleration force with other resistance forces, F_a represents air resistance force, F_{ro} the force from the load to the vehicle and F_{gr} represents the force of gravity given as;

$$F_{gr} = M_T g \sin \left(\tan^{-1} \left(\frac{\Delta h}{\Delta s} \right) \right) \quad (5)$$

Where F_{gr} represents the force of gravity, M_T represents the total mass of the vehicle, g represents the gravity constant, Δh represents the difference in heights between the flat road and the bump and Δs represents the change in slope of the road close to the speed bump. The inertia of the engine of the vehicle in motion is shown in Equation (6)

$$J_{eng} = \frac{W_{eng}}{dt} (T_{qeng} - T_{qclutch}) \quad (6)$$

Where J_{eng} represents the inertia of the engine, W_{eng} represents the weight of the engine, T_{qeng} represents the torque of the engine and $T_{qclutch}$ represents the torque of the clutch. The inertia for the vehicle was obtained and displayed in Equation 7.

$$J_{veh} = \frac{dt}{W_{clutch} T_{qclutch}} J_{eng} \quad (7)$$

Where J_{veh} represents the inertia of the vehicle, W_{clutch} represents the rotational velocity of the clutch when pedaled, $T_{qclutch}$ represents the clutch torque of the vehicle and dt represents the time.

When the vehicle comes in contact with the bumps, the height lift and force involved in container lift from the vehicle is shown in Equation 8 and Equation 9 respectively.

$$H_s = \frac{F_{decc} J_{veh}}{(M_T - M_c) g} \quad (8)$$

$$F_s = (M_T - M_c) g A_{dec} \quad (9)$$

Where H_s and F_s are the height of the toxic waste container above the vehicle and force taken to lift the container, M_c represents the mass of the vehicle and A_{dec} represents the overall deceleration of the vehicle with all the forces involved. Hence, the Weight of the toxic waste enclosed container on encountering the speed bump as transmitted by sensors 1 and 2 (internal sensors) is shown in Equation 10.

$$W_{B1,2} = V_B \frac{F_s}{dt} \quad (10)$$

Where W_B represents the weight of the container on encountering speed bump, V_B represents the velocity of the container during encounter with bumps and F_s represents the force of container lift when the vehicle passes through speed bump. The velocity of the vehicle V_B was given in Equation 11.

$$V_B = H_s A_{dec} - \frac{M_e + F_{decc}}{dt} \quad (11)$$

The determined velocity V_B was uniform for the four sensors, however, the weight of the container was uniformed for the two sensor placed at the edges close to the main vehicle ($W_{B1,2}$) at varying velocity and height of the bump. The weight of the container from the sensors placed at the end part of the vehicle ($W_{B3,4}$) is shown in Equation 12.

$$W_{B3,4} = W_{B1,2}H_s g \quad (12)$$

The A_{dec} and the H_s variation utilized for the determination of the V_B and $W_{B1,2}$, $W_{B3,4}$ is shown in Table 1;

Table 1; Deceleration and bump height data

S/N	Deceleration (A_{dec}) in m/s^2	Bump height (H_s) in m
1	2	0.02
2	2.5	0.02
3	3	0.02
4	2	0.03
5	2.5	0.03
6	3	0.03
7	2	0.04
8	2.5	0.04
9	3	0.04

For the speed bump scenarios, the various deceleration and bump considerations led to nine (9) variations for velocity and weight outcomes. Hence, plots was generated for the front and backend sensors for the velocity and the weight of the sensors at each deceleration and bump height combinations. The flow chart utilized for the modeling of the condition is shown in Figure 1.

The simulink model for the deceleration shown in Equation 2 was displayed in Figure 2. The simulink model for the equivalent total mass shown in Equation 3 was displayed in Figure 3. The simulink model for the deceleration force shown in Equation 4 was displayed in Figure 4. The simulink model for the engine inertia shown in Equation 6 was displayed in Figure 5. The simulink model of the Vehicle Inertia as shown in Equation 7 was displayed in Figure 6. The height of the container lift and the force for the container lift as shown in Equation 8 and Equation 9 were displayed in Figure 7 and Figure 8. The velocity for the first two sensors as shown in Equation 11 was displayed in Figure 9. The weight of the container for the two interior sensors as shown in Equation 10 was displayed in Figure 10. The weight transmitted by the exterior sensors as shown in Equation 12 was displayed in Figure 11.

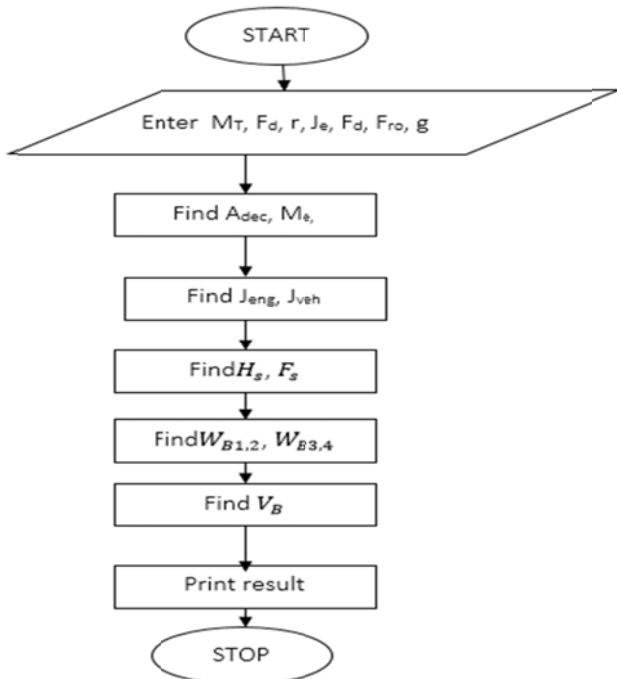


Figure 1; Flow diagram of the model of the trailer encounter with speed bumps obstruction while in motion

3.2.2 Simulink model of the Truck's encounter with Speed bumps

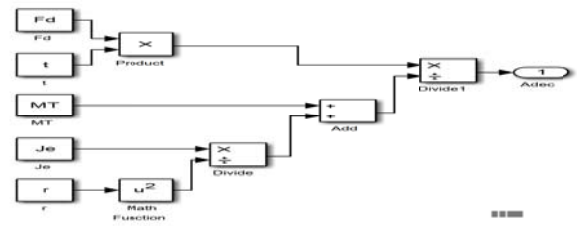


Figure 2 Simulink model for the deceleration

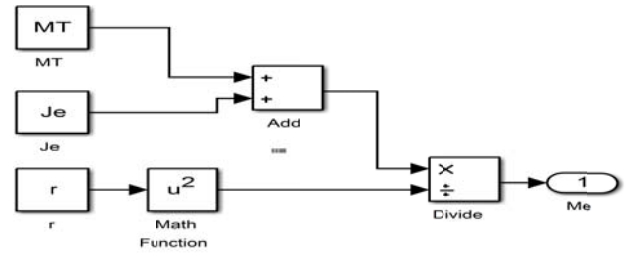


Figure 3 Simulink model for the equivalent mass of the vehicle with load

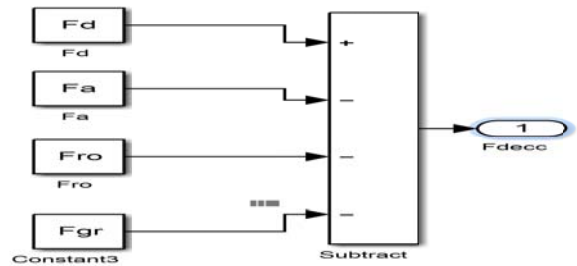


Figure 4 The simulink model for the deceleration force

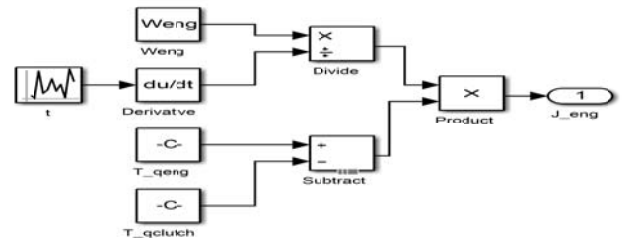


Figure 5 The simulink model for the Engine Inertia

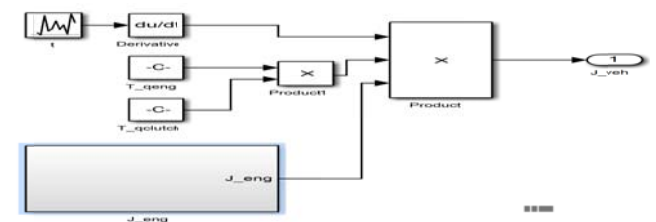


Figure 6 The simulink model for the vehicle inertia

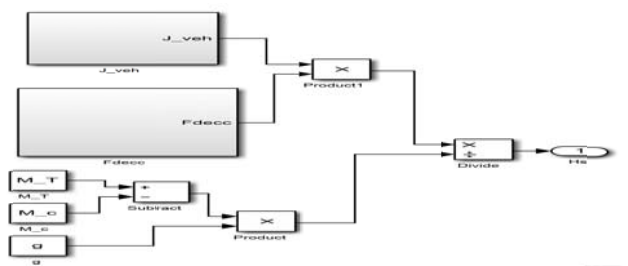


Figure 7 The simulink model for the height of container lift

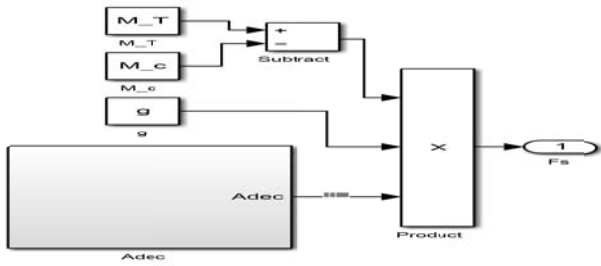


Figure 8 The simulink model for the force required for the container lift.

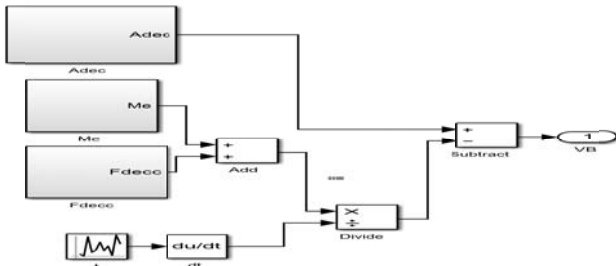


Figure 9 The simulink model for the velocity of the first two interior sensors

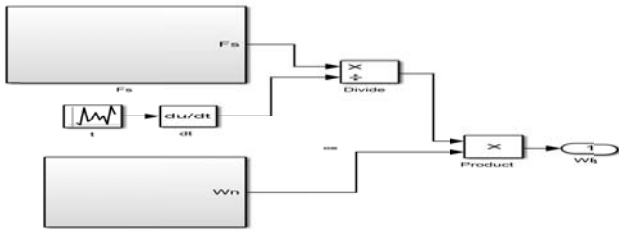


Figure 10 The simulink model for the weight transmitted by the interior sensors

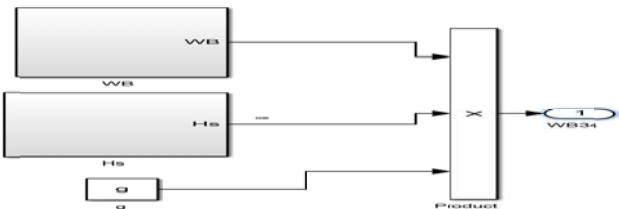


Figure 11 The simulink model for the weight of container from the back end sensors

3. RESULTS AND DISCUSSION

3.1 Results on the deceleration of the vehicle prior to the encounter with any obstruction

When the vehicle approaches a speed bump, the vehicle slows down. There was deceleration of the vehicle which occurred prior to the encounter with any obstruction and the response is shown in Figure 12. According to the results in Figure 12, the vehicle crossed the speed bumps at a deceleration of 3km/hr^2 .

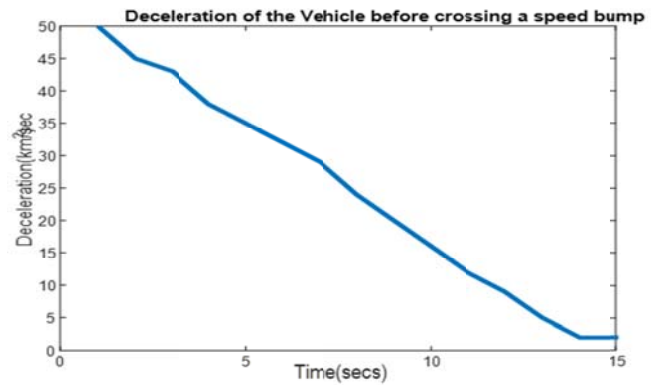


Figure 12; Deceleration of the Vehicle as it approaches a speed bump

3.2 Results on the equivalence mass of the vehicle on crossing the speed bump

The equivalence mass of the vehicle on crossing the speed bump is shown in Figure 13. The equivalence mass of the vehicle was increasing and reducing within the 15 seconds it crossed the speed bumps as shown in Figure 13.

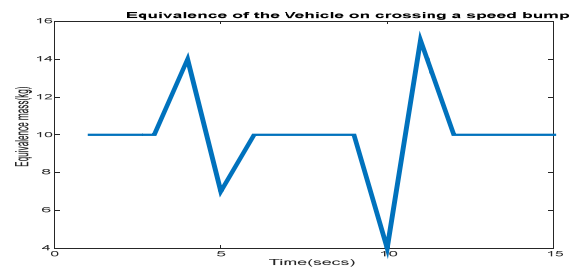


Figure 13; Mass equivalence of the vehicle on crossing the speed bump

3.3 Results on the deceleration force of the truck while crossing the obstruction

The deceleration force of the truck while crossing the obstruction is shown in Figure 14. The acceleration of the vehicle was lowered to enable smooth crossing of the obstruction and increased afterwards as shown in Figure 14. The force on the vehicle while crossing the bumps is shown in Figure 15. The gravitational force on the vehicle was reducing with deceleration of the vehicle and increased on crossing the obstruction as shown in Figure 16.

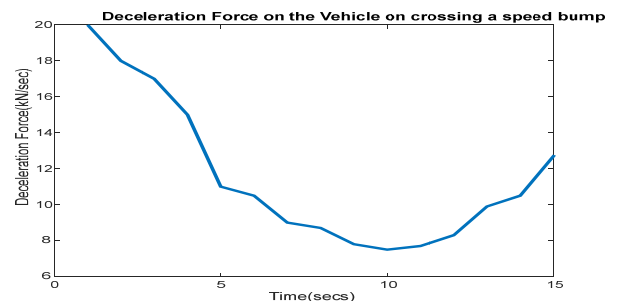


Figure 14; Deceleration force of the vehicle on crossing the speed bump

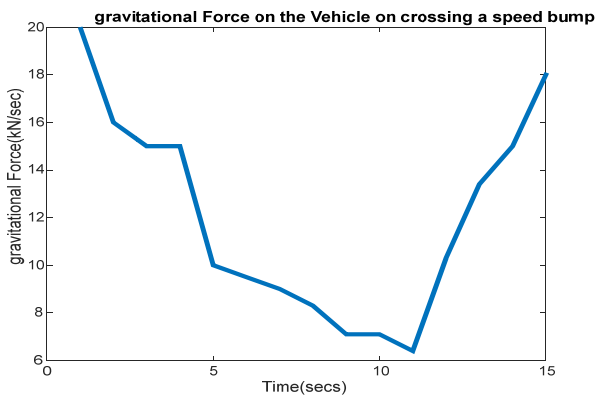


Figure 15, Gravitational force on the vehicle while crossing the speed bumps

3.4 Results on the rise height of the container from the base of the load carrier

The rise height of the container from the base of the load carrier is shown in Figure 16. The container rose to a height of 100 mm while the vehicle crossed the obstruction and the damping effect happened once and rested at zero due to the weight of the container. The force required for the container rise height is shown in Figure 17.

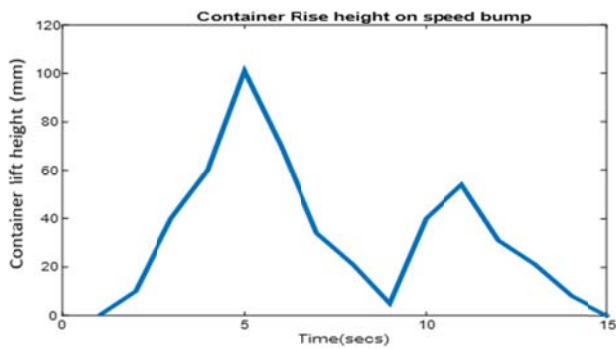


Figure 16; Container rise height from the base of the load carrier

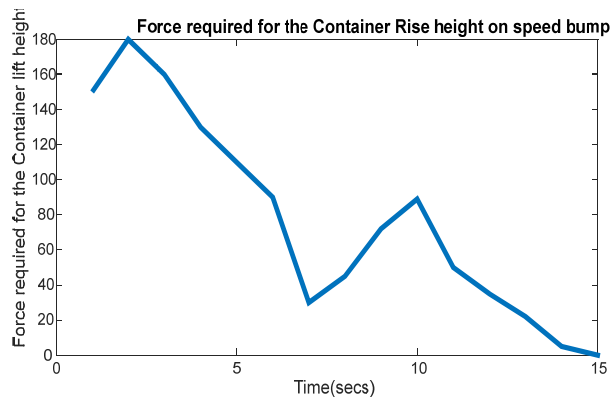


Figure 17; Force required for the container rise height

3.5 Results of the weights of the truck with the load from all the sensors at varying bump height and deceleration

The weights of the truck with the load from all the sensors 3 and 4 at deceleration of 3km/hr^2 and bump height of 0.04m is shown in the Figure 18 while weights of the truck with the load from all the sensors 1 and 2 at deceleration of 3km/hr^2 and bump height of 0.04m is shown in the Figure 19.

Similarly, the weights of the truck with the load from all the sensors 3 and 4 at deceleration of 2.5km/hr^2 and bump height of 0.04m is shown in the Figure 20 while weights of the truck with the load from all the sensors 1 and 2 at deceleration of 2.5km/hr^2 and bump height of 0.04m is shown in the Figure 21.

Again, the weights of the truck with the load from all the sensors 3 and 4 at deceleration of 2.0km/hr^2 and bump height of 0.04m is shown in the Figure 22 while weights of the truck with the load from all the sensors 1 and 2 at deceleration of 2.0km/hr^2 and bump height of 0.04m is shown in the Figure 23.

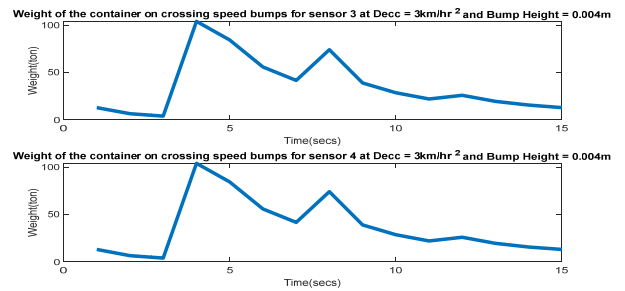


Figure 18; Weight of the container at deceleration of 3km/hr^2 and bump height of 0.04m for sensors 3 and 4

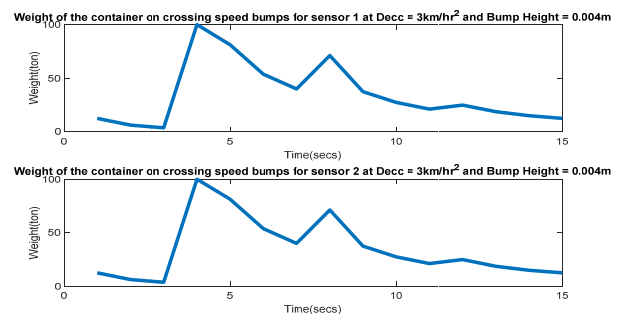


Figure 19; Weight of the container at deceleration of 3km/hr^2 and bump height of 0.04m for sensors 1 and 2

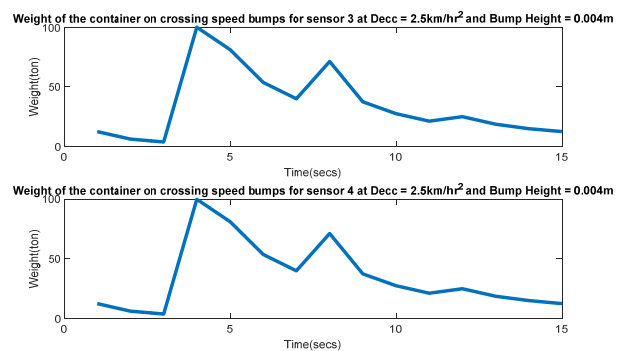


Figure 20; Weight of the container at deceleration of 2.5km/hr^2 and bump height of 0.04m for sensors 3 and 4

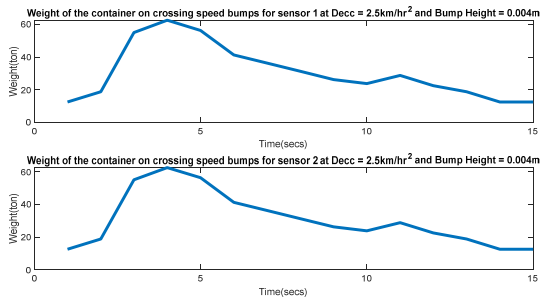


Figure 21; Weight of the container at deceleration of 2.5 km/hr² and bump height of 0.04m for sensors 1 and 2

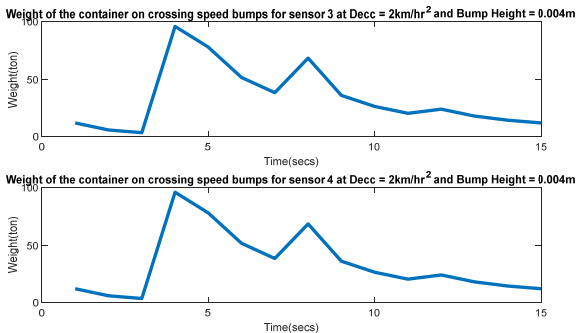


Figure 22; Weight of the container at deceleration of 2 km/hr² and bump height of 0.04m for sensors 3 and 4

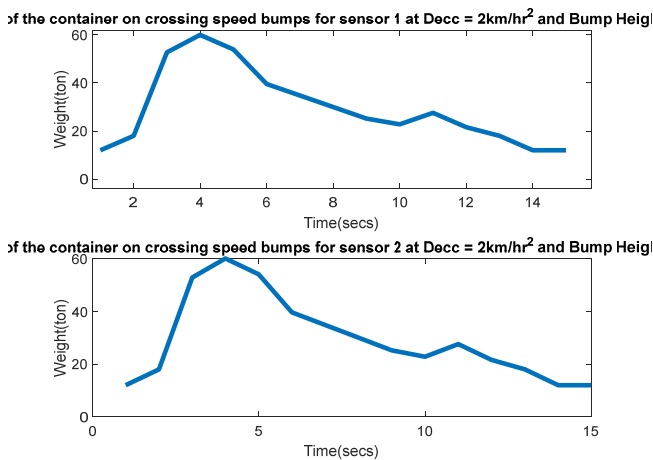


Figure 23; Weight of the container at deceleration of 2km/hr² and bump height of 0.04m for sensors 1 and 2

The weights of the truck with the load from all the sensors 3 and 4 at deceleration of 3km/hr² and bump height of 0.03 m is shown in the Figure 24 while weights of the truck with the load from all the sensors 1 and 2 at deceleration of 3km/hr² and bump height of 0.03 m is shown in the Figure 25.

Similarly, the weights of the truck with the load from all the sensors 3 and 4 at deceleration of 2.5 km/hr² and bump height of 0.03m is shown in the Figure 26 while weights of the truck with the load from all the sensors 1 and 2 at deceleration of 2.5 km/hr² and bump height of 0.03m is shown in the Figure 27. Again, the weights of the truck with the load from all the sensors 3 and 4 at deceleration of 2.0 km/hr² and bump height of 0.03m is shown in the

Figure 28 while weights of the truck with the load from all the sensors 1 and 2 at deceleration of 2.0 km/hr² and bump height of 0.03m is shown in the Figure 29.

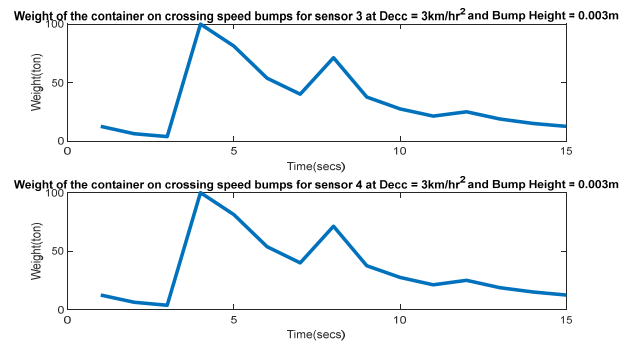


Figure 24; Weight of the container at deceleration of 3km/hr² and bump height of 0.03m for sensors 3 and 4

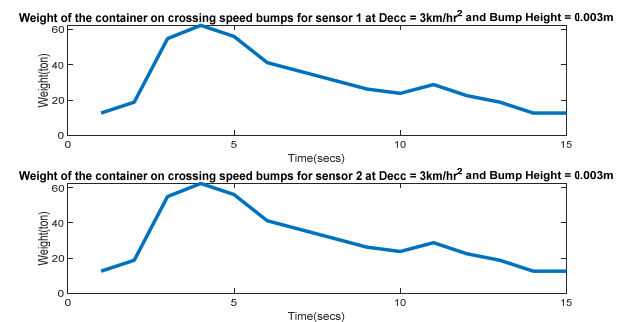


Figure 25; Weight of the container at deceleration of 3 km/hr² and bump height of 0.03m for sensors 1 and 2

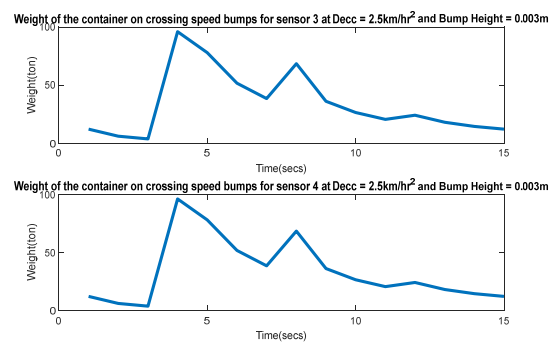


Figure 26; Weight of the container at deceleration of 2.5km/hr² and bump height of 0.03m for sensors 3 and 4

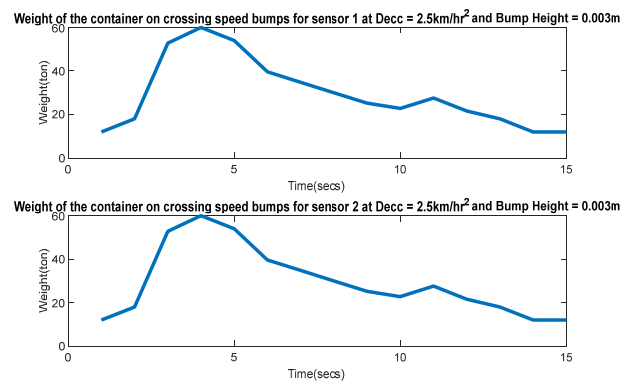


Figure 27; Weight of the container at deceleration of 2.5km/hr² and bump height of 0.03m for sensors 1 and 2

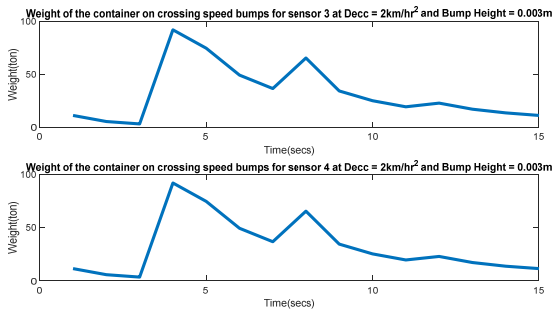


Figure 28; Weight of the container at deceleration of 2km/hr² and bump height of 0.03m for sensors 3 and 4

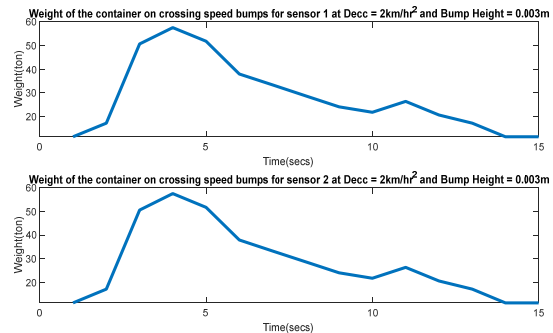


Figure 29; Weight of the container at deceleration of 2km/hr² and bump height of 0.03m for sensors 1 and 2
 The weights of the truck with the load from all the sensors 3 and 4 at deceleration of 3km/hr² and bump height of 0.02 m is shown in the Figure 30 while weights of the truck with the load from all the sensors 1 and 2 at deceleration of 3km/hr² and bump height of 0.02 m is shown in the Figure 31.

Similarly, the weights of the truck with the load from all the sensors 3 and 4 at deceleration of 2.5 km/hr² and bump height of 0.02m is shown in the Figure 32 while weights of the truck with the load from all the sensors 1 and 2 at deceleration of 2.5 km/hr² and bump height of 0.02m is shown in the Figure 33.

Again, the weights of the truck with the load from all the sensors 3 and 4 at deceleration of 2.0km/hr² and bump height of 0.02m is shown in the Figure 34 while weights of the truck with the load from all the sensors 1 and 2 at deceleration of 2.0 km/hr² and bump height of 0.02m is shown in the Figure 35.

From all the results on the variations in the weight of the toxic waste container displayed at varying deceleration and bump heights for all the sensors, it was noted that the increase in the deceleration and the bump height increase the weight of the container due to high landing at the process of crossing the bumps. Results on the velocity of the vehicle for the sensors are shown in Figure 36.

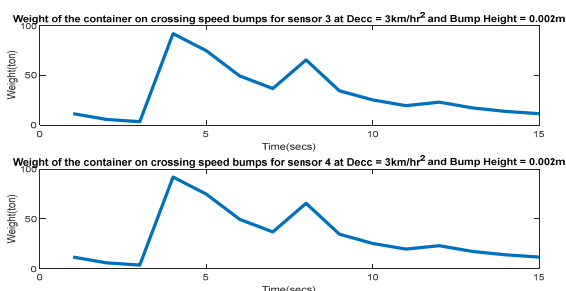


Figure 30; Weight of the container at deceleration of 3km/hr² and bump height of 0.02m for sensors 3 and 4

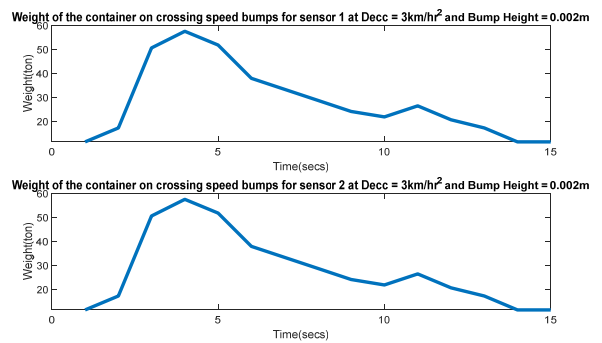


Figure 31; Weight of the container at deceleration of 3km/hr² and bump height of 0.02m for sensors 1 and 2

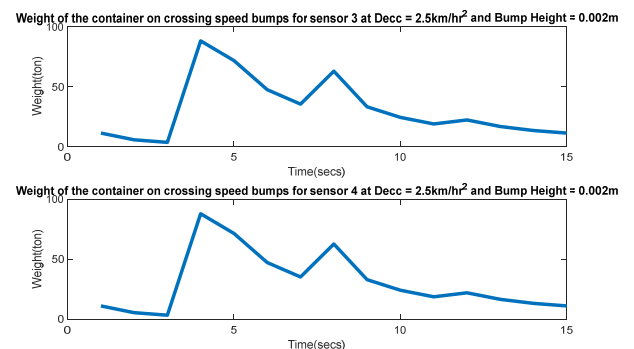


Figure 32; Weight of the container at deceleration of 2.5km/hr² and bump height of 0.02m for sensors 3 and 4

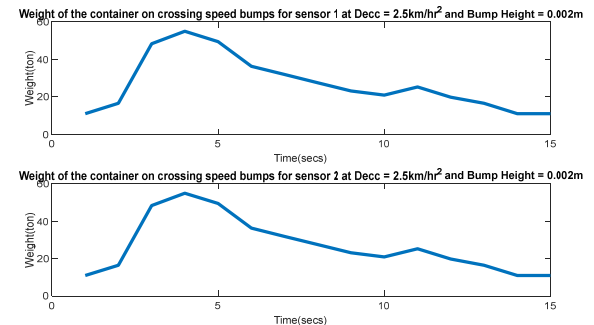


Figure 33; Weight of the container at deceleration of 2.5km/hr² and bump height of 0.02m for sensors 1 and 2

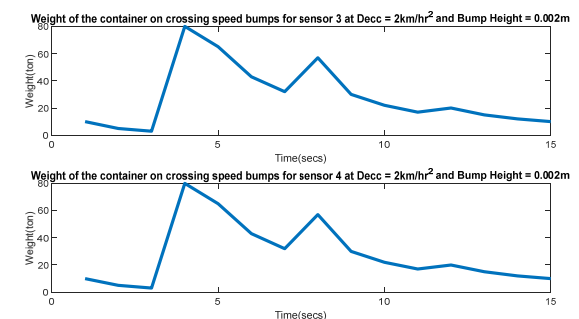


Figure 34; Weight of the container at deceleration of 2km/hr² and bump height of 0.02m for sensors 3 and 4

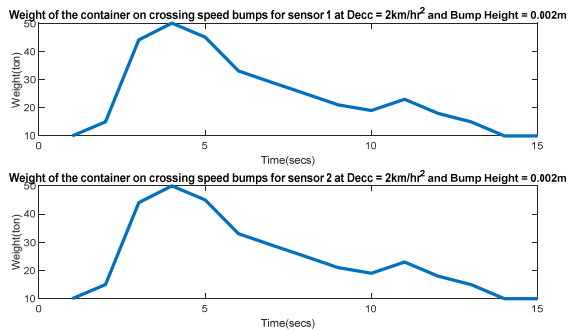


Figure 35; Weight of the container at deceleration of 2km/hr² and bump height of 0.02m for sensors 1 and 2

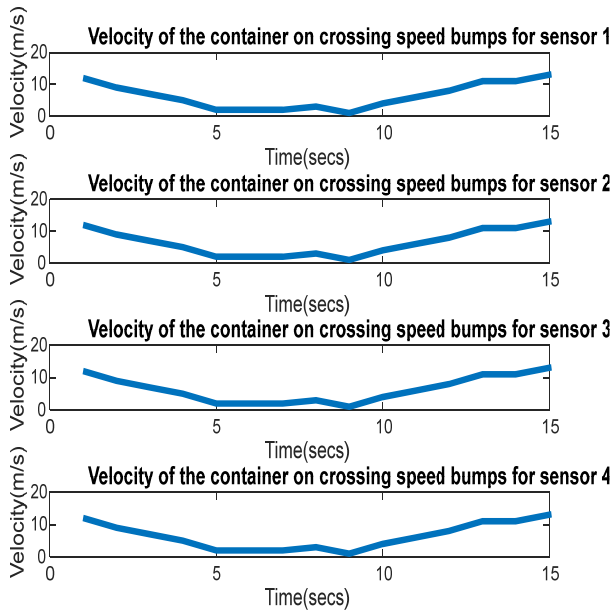


Figure 36; Velocity of the truck during obstruction as captured by the four sensors

4 CONCLUSION

Analytical models for evaluation of the variations in the solid waste container weight and velocity of the vehicle used in transportation of the toxic solid waste in the oil and gas industry are presented. The models are specifically meant for a situation where the vehicle encounters obstruction which in this work is the road bump obstruction. The essence of the study is to properly estimate the variations in the key parameters of the toxic solid waste container as the vehicle decelerates towards the road bump, as the waste container gets lifted while the vehicle hits the road and as the vehicle accelerates after the road bump. These parameters values variations are estimated so as to properly categorize the variations as encounter with speed bumps rather than tempering of the toxic waste. This study is particularly useful in the design of anti-tampering mechanism for application in smart toxic solid waste disposal management system.

The analytical models are further modelled in Simulink software and the simulations are conducted using sample solid waste container, sensors, and vehicle motion parameters. The variations in parameters like the container weight, vehicle velocity and acceleration before, during and immediately after the encounter with the road bump are captured and presented in graph plotted against time axis.

REFERENCES

- [1] Paiva, S., Ahad, M. A., Tripathi, G., Feroz, N., & Casalino, G. (2021). Enabling technologies for urban smart mobility: Recent trends, opportunities and challenges. *Sensors*, 21(6), 2143.
- [2] Bellini, P., Nesi, P., & Pantaleo, G. (2022). IoT-enabled smart cities: A review of concepts, frameworks and key technologies. *Applied Sciences*, 12(3), 1607.
- [3] Nižetić, S., Šolić, P., Gonzalez-De, D. L. D. I., & Patrono, L. (2020). Internet of Things (IoT): Opportunities, issues and challenges towards a smart and sustainable future. *Journal of cleaner production*, 274, 122877.
- [4] Li, C. H., Lee, T. T., & Lau, S. S. Y. (2023). Enhancement of municipal solid waste Management in Hong Kong through innovative solutions: a review. *Sustainability*, 15(4), 3310.
- [5] Villanueva, R. S. (2020). A pragmatic approach to improve the efficiency of the waste management system in Stockholm through the use of Big Data, Heuristics and open source VRP solvers: A real life waste collection problem; Stockholm's waste collection system and inherent vehicle routing problem, VRP.
- [6] Zeng, F., Pang, C., & Tang, H. (2024). Sensors on Internet of Things Systems for the Sustainable Development of Smart Cities: A Systematic Literature Review. *Sensors*, 24(7), 2074.
- [7] Isarin, N., Barteková, E., Brown, A., & Börkey, P. (2024). Digital Technologies for Better Enforcement of Waste Regulation and Elimination of Waste Crime.
- [8] Baker, M. A. (2021). *Waste Compliance and Tracking System (WCATS) Version 3 Requirements Document* (No. LA-UR-23-20072; EPC-WMP-WCATS-PLAN-002). Los Alamos National Laboratory (LANL), Los Alamos, NM (United States).
- [9] Kadus, T., Nirmal, P., & Kulkarni, K. (2020). Smart waste management system using IOT. *International Journal of Engineering Research and*, 9(04).
- [10] Shah, A. A. I., Fauzi, S. S. M., Gining, R. A. J. M., Razak, T. R., Jamaluddin, M. N. F., & Maskat, R. (2021). A review of IoT-based smart waste level monitoring system for smart cities. *Indonesian Journal of Electrical Engineering and Computer Science*, 21(1), 450-456.
- [11] Mookkaiah, S. S., Thangavelu, G., Hebbar, R., Haldar, N., & Singh, H. (2022). Design and development of smart Internet of Things-based solid waste management system using computer vision. *Environmental Science and Pollution Research*, 29(43), 64871-64885.
- [12] Murugesan, S., Ramalingam, S., & Kanimozhi, P. (2021). Theoretical modelling and fabrication of smart waste management system for clean environment using WSN and IOT. *Materials Today: Proceedings*, 45, 1908-1913.